

# NUMERICAL INVESTIGATIONS OF THE FATIGUE CRACK GROWTH UNDER SERVICE LOADING

H.A. Richard, M. Sander  
 University of Paderborn, Institute of Applied Mechanics  
 Pohlweg 47-49, D-33098 Paderborn, Germany  
 sander@fam.upb.de

## Abstract

During the fatigue crack growth acceleration and retardation effects occur due to service loadings. These effects lead to lifetime reductions as well as to lifetime extensions of real structures. In order to understand these interaction effects numerical investigations have been performed for different loading cases. Within the scope of this paper at first the finite element modelling and secondly, the results of the finite-element analyses are shown. The residual stress distribution shows that at the location of the loading change strong compressive stresses are caused, which are the result of strong plastic deformations. The amount of the plastic deformation and therefore the residual stresses are influenced by the overload or block loading ratio, the baseline level loading, the state of stress and the amount of mode II. With the calculation of an opening stress intensity factor  $K_{op}$  by the numerical simulations an effective cyclic stress intensity factor and further the crack growth rate can be calculated by a combined model. The predicted crack velocities are in good agreement with corresponding experimental results.

## Introduction

During the working time components and structures are exposed to a service loading, i.e. a variable amplitude loading in general. Thereby during the fatigue crack growth both acceleration and retardation effects occur.

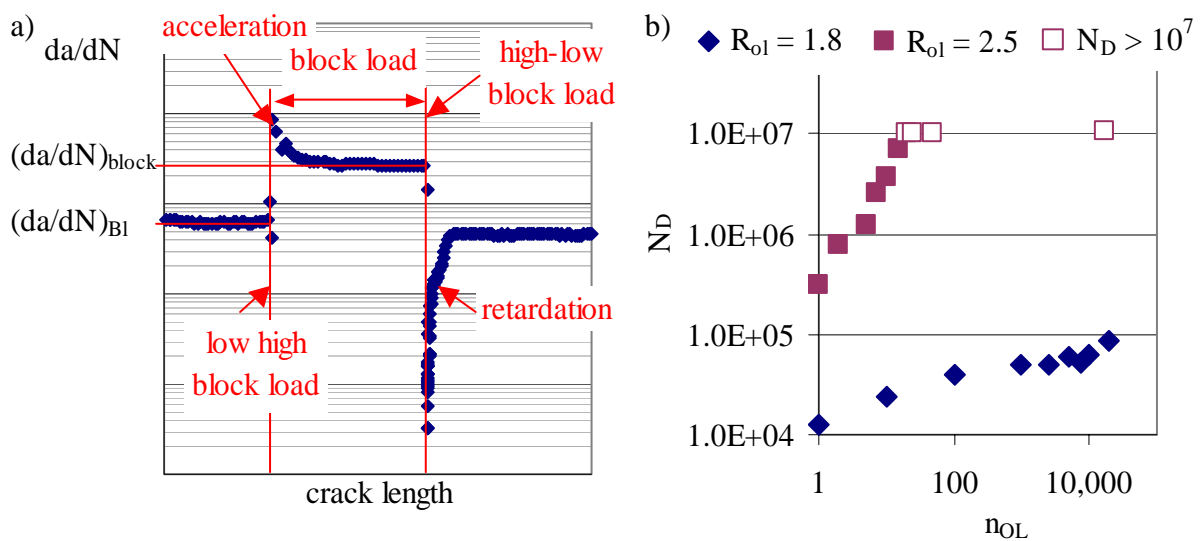


Figure 1: a) Acceleration and retardation effects due to a block load  
 b) Delay cycles  $N_D$  due to single and multiple overloads as well as block loads in dependence of the number of interspersed overloads  $n_{ol}$  and the overload ratio  $R_{ol}$

Fig. 1a shows the crack growth rates before, during and after a block load. It becomes apparent that due to the low-high block load an acceleration effect, but due to the high-low block load a strong retardation effect appears. Both the accelerated and the retarded fatigue crack growth depends on the block load ratio  $R_{\text{Block}} = K_{\text{Block}}/K_{\text{Bl,max}}$ , the baseline level loading and the R-ratio. Furthermore the retardation effect is influenced by the number  $n_{\text{ol}}$  of interspersed overloads. In Fig. 1b the number of delay cycles  $N_{\text{D}}$ , which are necessary to obtain the same crack growth rate as before the overload at constant amplitude loading, are illustrated in dependence of the interspersed overloads with overload ratios  $R_{\text{ol}} = K_{\text{ol}}/K_{\text{Bl,max}}$  of 1.8 and 2.5. With an increasing number of interspersed overloads the number of delay cycles increase up to a limit value, i.e.  $N_{\text{D}}$  converges against a constant value depending on the overload ratio. Moreover it can be seen that high-low block loads lead to larger retardation effects than single overloads. Besides the overload ratio and the baseline level loading also the loading direction influences the retardation effect after overloads. Within the scope of this paper the results of finite element analyses are presented in order to investigate the reasons for these so-called interaction effects.

### Finite element simulation of variable amplitude loading

For the finite element analyses using ABAQUS<sup>TM</sup>/Standard the CTS (Compact Tension Shear) specimen developed by Richard [1] is used in order to investigate mode I, mixed mode and mode II loading situation.

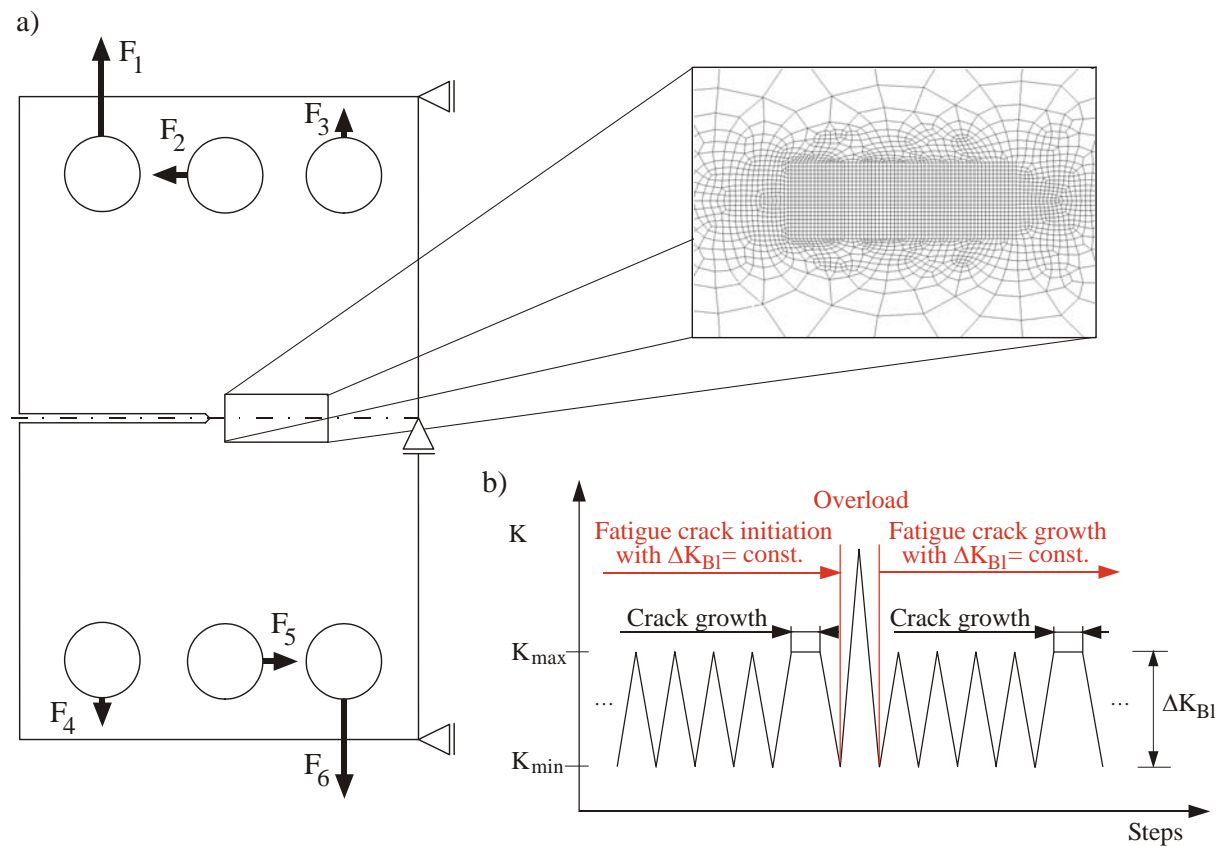


Figure 2: a) Loading and bearing of the used CTS specimen and a section of the Finite-element-mesh in the interesting region  
b) Release node concept of the FE-simulation of the fatigue crack growth

Fig. 2 shows the used CTS specimen with the appropriate loading and bearing of the FE-model. Depending on the mixed mode ratio the corresponding forces  $F_1$  to  $F_6$  have to be adapted [1]. In the region of the crack growth a rectangular mesh with quadratic 4-node elements with an element length of 0.025 mm is chosen. In order to consider the plastic deformations an elastic-plastic material behaviour is modelled, whereby the monotonic stress-strain curve of the used aluminium alloy 7075 T651 is applied with nonlinear kinematic hardening [2, 3].

For the investigations of the crack closure the surfaces along the crack line are defined as contact surfaces, whereby the master-slave-algorithm of ABAQUS is used [4]. Along the arising crack path the nodes are bonded at the beginning. During the simulation the nodes are debonded successively over a distance of 0.1 mm in order to realize the fatigue crack growth (Fig. 1b). In literature several release node concepts are described [5-8]. Within the scope of this paper the nodes are released at maximum applied baseline level loading according to Newman's concept [5], but in order to ensure stabilized hysteresis loops five cycles are positioned between each crack growth step.

The FE-analyses are performed with a constant baseline level loading  $\Delta K_{BI} = 7 \text{ MPam}^{1/2}$  and a constant stress ratio of the baseline level loading  $R_{BI} = 0.1$ , i.e. after each crack growth step the forces  $F_1$  to  $F_6$  have to be adapted to the current crack length according to Richard's definitions of the stress intensity factors for the CTS specimen [1-3]. After the generation of a fatigue crack of 0.5 mm in order to obtain the current residual stresses [9, 10] at 50.0 mm a single mode I, mixed mode or mode II overload as well as a mode I block load are interspersed. Afterwards a mode I baseline level loading is applied again.

## Residual stresses and crack opening due to overloads

For the investigations of the reasons for the retardation effects after single overloads mode I, mixed mode and mode II overloads with different overload ratios  $R_{ol} = K_{V,ol}/K_{BI,max}$  are interspersed into a constant baseline level loading of  $7 \text{ MPam}^{1/2}$ . Richard [1] defines the comparative stress intensity factor  $K_{V,ol}$  as follows

$$K_{V,ol} = 0.5K_{I,ol} + 0.5\sqrt{K_{I,ol}^2 + 5.34K_{II,ol}^2} \quad (1)$$

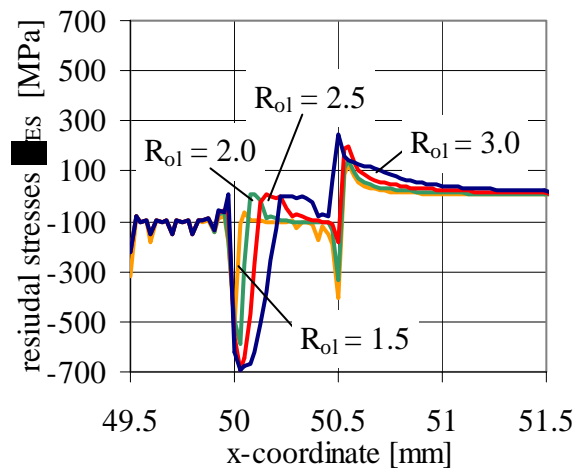


Figure 3: Residual stresses 0.5 mm after an mode I overload depending on the overload ratio  $R_{ol}$

The effect of a mode I overload on the residual stresses  $\sigma_{ES}$  at a crack length of 50.5 mm depending on the overload ratio  $R_{ol}$  is presented in Fig. 3. It becomes obvious that depending on the overload ratio high compressive residual stresses at the crack flanks are caused due to the overload. With an increasing overload ratio the residual stresses increase up to a value of approximately -700 MPa. If this limit is reached the residual stresses are extended over a larger distance of the crack surface. But not only the residual stresses behind the crack tip are disturbed, but also  $\sigma_{ES}$  in the ligament. Further investigations have shown that even the stress distribution in y-direction is changed [2]. The reason for these modifications of the stress distributions

are the plastic deformations caused by the overload. Due to the overload plastic deformations, so-called humps are built, which cause a complete or partial crack closure. This means that the crack is closed before the minimum load is reached and remains closed up to a certain load level, respectively. In Fig. 4a the crack opening 0.5 mm after a mode I overload ( $R_{ol} = 2.5$ ) at maximum baseline level loading with symmetrical humps compared to a fatigue crack under constant amplitude loading is shown. By applying a mixed mode overload with the same overload ratio  $R_{ol} = 2.5$  the shape as well as the size of the plastic zone is affected [2, 3]. With an increasing amount of mode II of the overload the plastic zone size is enlarged and rotated, but the humps are smaller. Moreover as a result of the changed plastic zone orientation mixed mode overloads lead to an asymmetrical crack opening. Fig. 4b-d illustrates the crack opening by means of the y-displacements 0.5 mm after mixed mode and mode II overloads. The smaller plastic deformations and thus the smaller residual stresses are the reason for the smaller retardation effect observed in corresponding experiments [11].

In addition to the overload ratio and the fraction of shear loading of the overload also the baseline level loading influences the residual stresses and the crack opening. The numerical results are also affected by the chosen state of stress [2, 3].

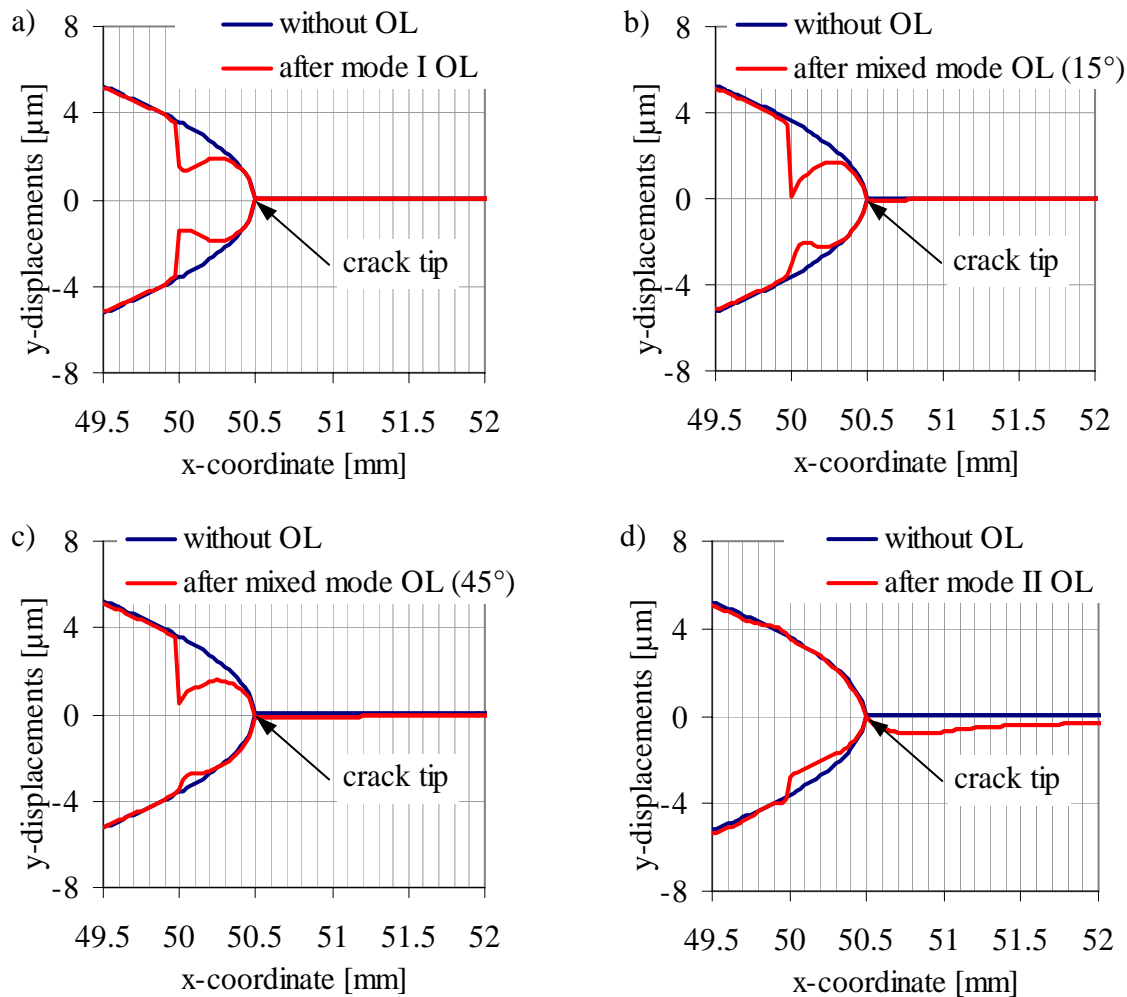


Figure 4: Comparison of the fatigue crack opening without and with an overload  $R_{ol} = 2.5$  at a crack length of 50.5 mm with

- a)  $K_{II,ol}/(K_{I,ol}+K_{II,ol}) = 0$  (mode I OL)      b)  $K_{II,ol}/(K_{I,ol}+K_{II,ol}) = 0.106$  ( $\alpha = 15^\circ$ )  
c)  $K_{II,ol}/(K_{I,ol}+K_{II,ol}) = 0.306$  ( $\alpha = 45^\circ$ )      d)  $K_{II,ol}/(K_{I,ol}+K_{II,ol}) = 1$  (mode II OL)

### Comparison of simulation results of block loads and overloads

For the investigations of low-high-low block loads after the generation of a fatigue crack of 0.5 mm a block load with an block load ratio of 2.0 is interspersed, whereby the minimum stress intensity factor is kept constant. The block load ends at  $a = 50$  mm after a block length of 0.5 mm so that the high-low transition is at the same crack length as the aforementioned overloads.

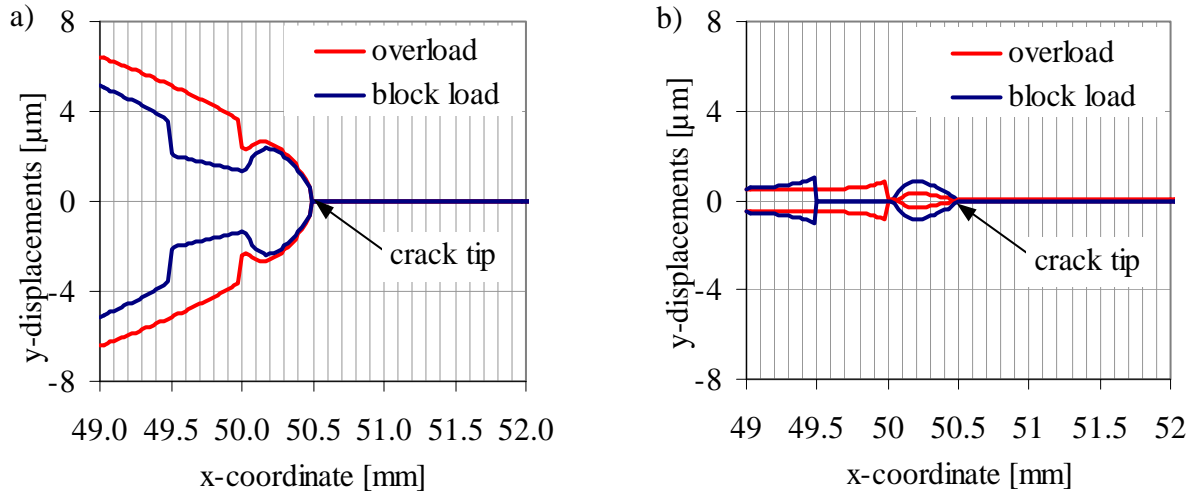


Figure 5: Crack opening and crack closure 0.5 mm after a single overload and a block load a) at  $K_{Bl,max}$  and b) at  $K_{Bl,min}$

Fig. 5a exemplifies a comparison of the crack openings at maximum baseline level loading 0.5 mm after an overload and a block load, respectively. In contrast to a single overload plastic deformations remain over a larger distance of the crack flanks, which reflect the length of the block load.

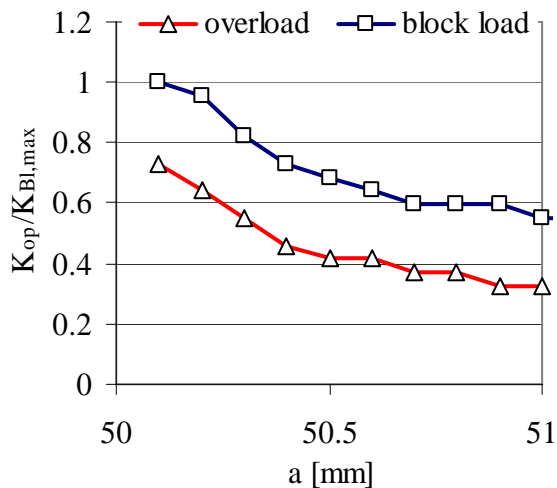


Figure 6: Relation of the crack opening stress intensity factor  $K_{op}$  and the maximum baseline level loading after overloads and block loads in dependence of the crack length

This hump lead at minimum baseline level loading to a complete or a partial crack closure after a certain crack growth. In Fig. 5b the unloading situation at  $K_{Bl,min}$  is illustrated. It becomes apparent that the crack is closed in the far-field over the distance of the overload or the block load, while the crack tip is opened. At a crack length of 50.5 mm the crack tip is opened wider after a block load than after an overload. However, it has to be mentioned that at 51.0 mm the crack tip after an overload is opened wider [2]. The crack before the service load is opened as well.

In order to quantify the crack closure a crack opening stress intensity factor  $K_{op}$  is determined.  $K_{op}$  is defined as the minimum stress intensity factor, at which along the crack surfaces no contact exists anymore. Fig. 6 shows the relation between  $K_{op}$  and the

maximum baseline level loading  $K_{Bl,max}$  in dependence of the crack length. With a growing crack  $K_{op}/K_{Bl,max}$  decreases until at a certain crack length a constant value of the constant amplitude loading is reached. Besides it can be seen that the high-low block load lead to higher  $K_{op}/K_{Bl,max}$  values, i.e. with  $K_{Bl,max} = const.$  the crack opening stress intensity factors are higher. Moreover it can be concluded that the influenced crack length after a block load is larger than after an overload, which can be observed in appropriate experiments [2].

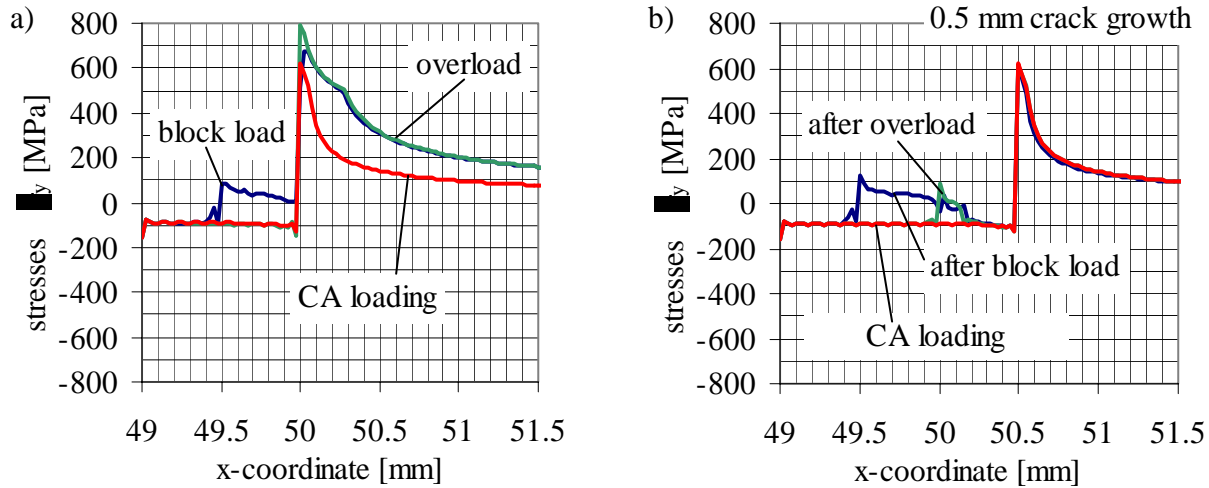


Figure 7: Comparison of the  $\sigma_y(x)$  stress distribution of a constant amplitude (CA) loading with the stress distribution after an overload and a high-low block load ( $R_{ol} = R_{block} = 2.0$ )  
 a) during the overload or the high-low block load at  $a = 50.0$  mm and  
 b) at maximum baseline level loading at  $a = 50.5$  mm

Due to the changed plastic deformations also the stress distributions are different. Fig. 7a shows the  $\sigma_y(x)$  stress distribution of a constant amplitude loading compared to the stresses during an overload or a high-low block load at a crack length of 50.0 mm.

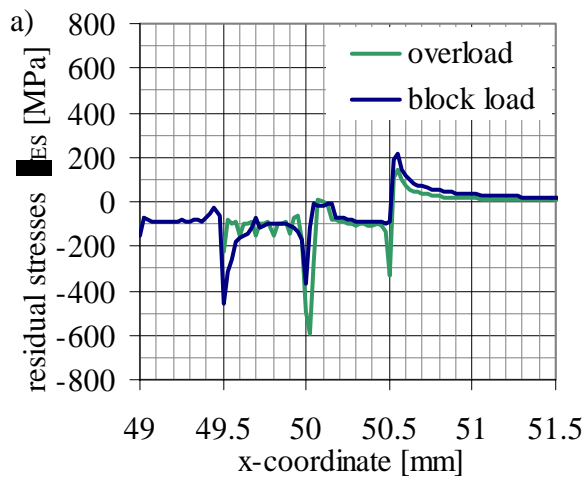


Figure 8: Residual stresses after an overload and a block load at 50.5 mm

It becomes apparent that the stresses in the ligament during the block load are nearly identical with the stresses during the overload, which are noticeably higher than those of the constant amplitude loading. At the crack flanks tensile stresses are produced by the block load contrary to compressive stresses of the constant amplitude loading. Due to the overload also tensile stresses are caused, which can be observed after 0.5 mm crack growth (Fig. 7b).

The different effects of the overload or the block load on the fatigue crack growth also can be seen by means of the residual stresses at a crack length of 50.5 mm (Fig. 8). At the points of the loading change the residual stresses are disturbed. Obviously the retardation effect of the high-low block load has not vanished, because the residual stresses in the ligament are still different from those after the overload, which are equal to the ones of the constant amplitude loading at this crack length [2].

## Combined crack growth model

Due to the plastic deformations along the crack surfaces and the elevated residual stresses as a result of overloads and block loads the crack opening stress intensity factors  $K_{op}$  are modified. The crack closure leads to an effective cyclic stress intensity factor

$$\Delta K_{eff} = K_{max} - K_{op}, \quad (1)$$

whereby the  $K_{op}$  values are determined by numerical analyses. With the approach of Erdogan and Ratwani [12]

$$\frac{da}{dN} = \frac{C(\Delta K_{eff} - \Delta K_{th})^m}{(1-R)K_{IC} - \Delta K_{eff}} \quad (2)$$

crack growth rates can be calculated. Fig. 9 shows the characteristics of the crack velocity of a low-high-low block load experiment compared to the numerically determined crack growth rates depending on the state of stress. The crack velocities are underestimated by the FE-analysis with plain stress and overestimated by the FE-analysis with plain strain conditions.

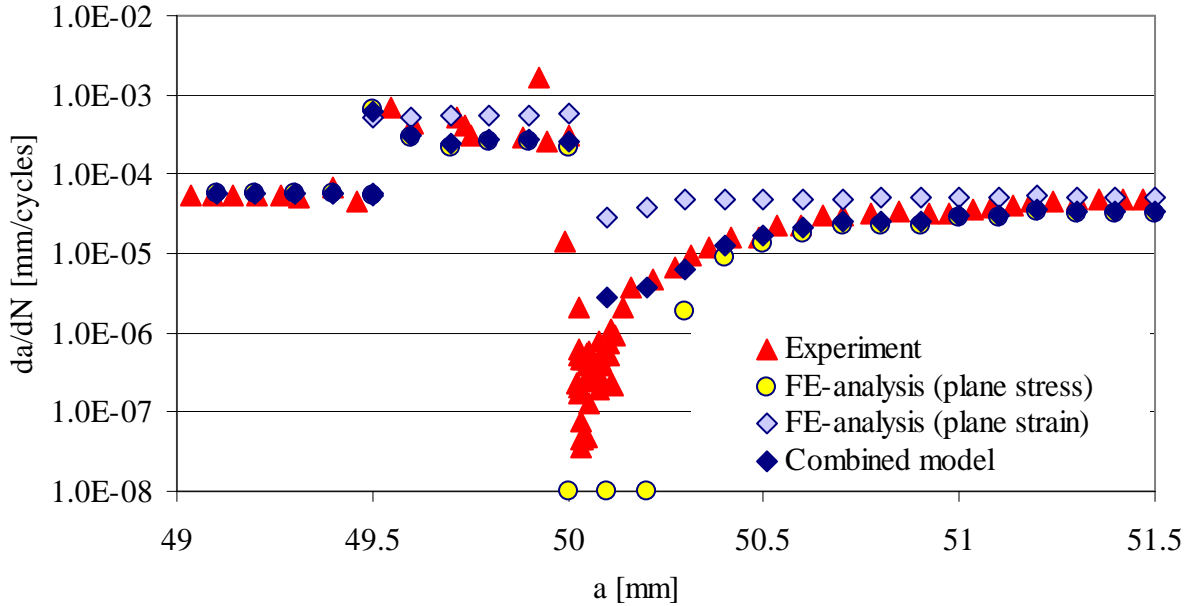


Figure 9: Crack growth rate of a block load experiment in comparison to computed crack velocities depending on the state of stress

Because in components and structures a combined state of stress consisting of both plane stress and plane strain is present, Sander developed a combined model [2], which is defined as follows:

$$\frac{da}{dN} = \alpha_{CF} \left( \frac{da}{dN} \right)_{plane\ stress} + (1 - \alpha_{CF}) \left( \frac{da}{dN} \right)_{plane\ strain}, \quad (2)$$

whereby  $\alpha_{CF}$  is a constraint factor.

The crack growth calculated with the combined model are in good agreement with the experimental data shown in Fig. 9. By means of the numerical simulations even the small acceleration phase at the beginning of the low-high block load as well as the large retardation

effect after the high-low block are accurately described. Also the predictions of the constant amplitude loading are in good agreement with the experiments.

Moreover also good results are obtained with Sander's combined model for the prediction of overloads with different overload and mixed mode ratios. A comparison shows that both the initial acceleration and the retardation effect after the overload are realised [2].

## Conclusion

In literature several reasons for interaction effects during the fatigue crack growth after overloads and block loads are discussed. Within the scope of this paper it has been shown that due to overloads and block loads plastic deformations occur, which lead to crack closure and modifications in the stress distributions ahead and behind the crack tip. This effect is influenced by the overload ratio and the baseline level loading as well as by the amount of mode II of the overload. Moreover it can be concluded that the state of stress has a significant influence on the simulation results. With Sander's combined model crack growth rates can be computed, which are in good agreements with experimental data.

## References

1. Richard, H.A., *Bruchvorhersagen bei überlagerter Normal- und Schubbeanspruchung von Rissen (Fracture predictions of cracks under superimposed normal and shear loading)*, VDI-Forschungsheft 631/85, VDI-Verlag, 1985, in german
2. Sander, M., *Einfluss variabler Belastung auf das Ermüdungsriswachstum in Bauteilen und Strukturen (Influence of variable amplitude loading on the fatigue crack growth in components or structures)*, VDI-Verlag, 2003, in german.
3. Sander, M., Richard, H.A., *Intern. Journal of Fatigue*, will be published.
4. Hibitt, Karlsson & Sorensen, *ABAQUS/Standard users's manual*, Version 5.8, Pawtucket, Rhode Island, 1998
5. Newman, J.C., In *Fatigue 2002* edited by A.F. Blom, vol. **1**, EMAS, Stockholm, 2002, pp. 55-70.
6. McClung, R.C., Sehitoglu, H., *Engineering Fracture Mechanics*, Vol. **33**, 1989, pp. 237-252.
7. Ogura, K., Ohji, K., *Engineering Fracture Mechanics*, Vol. **9**, 1977, pp. 471-480.
8. Anquez, L., In: *Fatigue crack growth under variable amplitude loading* edited by J. Petit et al., Elsevier Applied Science, London, 1988, pp. 194-207.
9. Wang, H., Buchholz, F., Richard, H., Jägg, S., Scholtes, B., *Computational Materials Science*, Vol. **16**, 1999, pp. 104-112.
10. Zhang, X., Chan, A.S.L., Davies, G.A.O., *Engineering Fracture Mechanics*, Vol. **42**, 1992, pp. 305-321.
11. Sander, M., Richard, H.A., *Intern. Journal of Fatigue*, Vol. **25**, 2003, pp. 999-1005.
12. Erdogan, F., Ratwani, M., *Intern. Journal of Fracture Mechanics*, vol. **6**, 1970, pp. 379-392.